

Dark Acoustic Oscillations and the Hubble Tension

Mathias Garny^{1,*}, Florian Niedermann^{2,†} and Martin S. Sloth^{3‡}

¹*Physik Department T31, School of Natural Sciences, Technische Universität München
James-Frank-Straße 1, D-85748 Garching, Germany*

²*Nordita, KTH Royal Institute of Technology and Stockholm University
Hannes Alfvéns väg 12, SE-106 91 Stockholm, Sweden*

³*Universe-Origins, University of Southern Denmark,
Campusvej 55, 5230 Odense M, Denmark*

Abstract

The Hubble tension and the recently reported anomaly in data from the Dark Energy Spectroscopic Instrument (DESI) are considered to pose serious challenges to the standard Λ CDM model of cosmology. In this work, we show that resolving the Hubble tension with a scenario featuring dark radiation–matter decoupling (DRMD) predicts the presence of dark acoustic oscillations (DAO) similar in scale to baryon acoustic oscillations (BAO). Using an inference independent of large-scale structure data, relying only on Planck measurements of the cosmic microwave background and SH0ES-calibrated supernova data, we find evidence for a DAO signal with drag-horizon scale $r_{d,\text{DAO}} \in [54, 65] \text{ Mpc}/h$ (68% C.I.) and amplitude $A_{\text{DAO}} \in [0.02, 0.05]$ (68% C.I.). These predictions provide a concrete target for current and upcoming large-scale structure surveys, including DESI, Euclid, and the Roman Space Telescope. Remarkably, the predicted DAO properties are consistent with those required to explain the DESI anomaly, offering both an alternative to evolving dark energy and a preliminary validation of the relevance of a dark radiation–matter decoupling scenario for addressing the Hubble tension.

* mathias.garny@tum.de

† florian.niedermann@su.se

‡ sloth@sdu.dk

I. INTRODUCTION

Observational challenges to Λ CDM, the standard model of cosmology, have emerged from high-precision cosmic microwave background (CMB), baryon acoustic oscillations (BAO), and supernova (SN) observations. In this work, we focus on the two most significant challenges and argue that they provide two independent pieces of evidence pointing to the same underlying new physics beyond Λ CDM, sharpening arguments made recently in [1, 2].

The first challenge is the Hubble tension. The expansion rate of the Universe today measured directly by using standard candles disagrees with the expansion rate predicted in the Λ CDM model when fitted to CMB and BAO data. The most precise measurement of the expansion rate today from the SH0ES collaboration obtains $H_0 = 73.04 \pm 1.04$ km/s/Mpc [3], while the expansion rate inferred from the CMB, when assuming the Λ CDM model, implies $H_0 = 67.36 \pm 0.54$ km/s/Mpc [4] when using Planck CMB data. These observational determinations of H_0 are in about 5σ conflict with each other. While one may wonder if there is unknown systematics affecting these measurements, which could explain this disagreement within the Λ CDM model, one should keep in mind that several measurements of the local expansion rate using different standard candles agree with the supernova measurement of SH0ES¹. At the same time, BAO measurements, combined with a constraint on the amount of baryons from Big Bang nucleosynthesis (BBN), agree with the CMB measurement [6] only if Λ CDM is assumed. For this reason, we will focus on explanations of the Hubble tension, which involves new physics going beyond Λ CDM (for reviews of the tension and proposed solutions see [7–9]).

The second challenge, which we refer to as *DESI anomaly*, is related to recent high-precision BAO measurement of the Dark Energy Spectroscopic Instrument (DESI). When DESI data is combined with Planck CMB [4] and Pantheon+ supernova measurements [10, 11], one finds a 2.8σ preference for a model with evolving dark energy parametrized as a two-parameter extension of Λ CDM. Specifically, if the dark energy equation-of-state parameter is assumed to take the form $w(a) = w_0 + w_a(1 - a)$, where Λ CDM corresponds to $w_0 = -1$, $w_a = 0$, DESI finds [6] $w_0 = -0.838 \pm 0.055$, $w_a = -0.62_{-0.19}^{+0.22}$. This interpretation is however unsettling as the preferred values would imply that dark energy entered a phantom regime with $w < -1$ in the recent past, although attempts to avoid this interpretation in terms of

¹ For a recent review of local H_0 measurements, see [5].

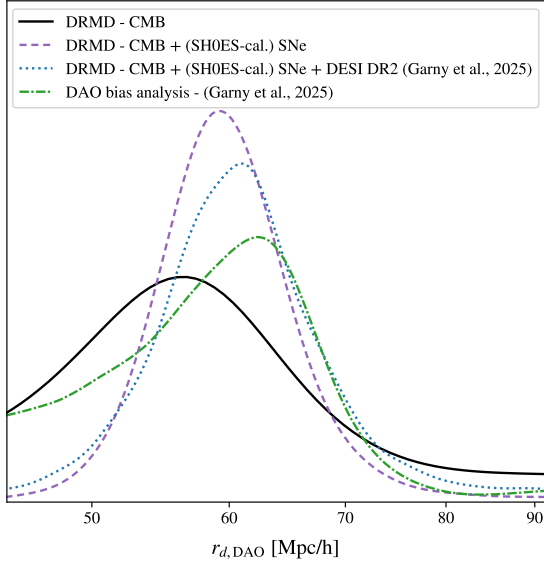


FIG. 1. 1D posterior of the dark drag horizon, $r_{d,\text{DAO}}$, from CMB alone (Planck 2018 temperature, polarization, and lensing) and from CMB combined with calibrated supernovae (Pantheon+ and SH0ES prior on the absolute magnitude M). Also shown are the corresponding posteriors from the four-parameter DRMD analysis of Ref. [1] (including DESI DR2) and the DAO bias study of Ref. [2]. All curves are normalized to the same integral over the plotted interval. The compatibility of all curves with a value around $60 \text{ Mpc}/h$ is one of the main results of this work. For reference, the baryon drag horizon is centred around $100 \text{ Mpc}/h$.

interacting dark energy and dark matter have been made [12–19].

Another reason to find evolving dark energy unsettling as an explanation of the DESI anomaly is that evolving dark energy does not address the Hubble tension. The BAO experiments measure the product of the expansion rate H_0 and the sound horizon at baryon decoupling $r_{d,\text{BAO}}$, which is measured by DESI to be $H_0 \cdot r_{d,\text{BAO}} = 101.54 \pm 0.73$ ($100 \text{ km})/\text{s}$ [6]. This means, that in order to stay consistent with BAO measurements, any solution to the Hubble tension that fits the CMB with a higher value of H_0 needs to involve new physics before decoupling in order to also lower $r_{d,\text{BAO}}$, and thus remain compatible with BAO measurements [20, 21]. This also implies that late-time evolving dark energy cannot resolve the Hubble tension.

One of the simplest ideas for new physics before recombination, which could lower the sound horizon and alleviate the Hubble tension, while staying compatible with BAO measurements, is dark radiation. Dark radiation would maintain a constant energy density rela-

tive to ordinary radiation in the radiation dominated epoch, and redshift away compared to the total energy density after matter-radiation equality shortly before recombination. This would lower the sound horizon and raise H_0 while minimizing its effect on structure formation in the late Universe. But if the dark radiation is free-streaming, it induces anisotropic stress and enhances diffusion damping on small scales in the CMB [22] (predominantly scales that enter the horizon before matter-radiation equality) beyond an acceptable level. To avoid these problems, it is natural to consider a component of self-interacting dark radiation (SIDR), which behaves like a tightly coupled fluid, and is not free-streaming [23–28].

There are two basic problems with SIDR as a solution to the Hubble tension in its simplest form. First, it is ruled out by BBN [29], which puts a rather stringent bound on any form of dark radiation. In order to alleviate the Hubble tension, an amount of SIDR, which corresponds to an extra amount of relativistic degrees of freedom $\Delta N_{\text{eff}} \gtrsim 0.5$, is needed, which is ruled out by BBN constraints. Second, even when ignoring BBN constraints, and allowing for $\Delta N_{\text{eff}} \gtrsim 0.5$, SIDR does not provide a full resolution of the Hubble tension, but only reduces the tension to around 3σ when using Planck 2018 CMB data [1, 30]. The latest constraints from ACT provide even stronger constraints on extra relativistic degrees of freedom [31] (see section IV for a discussion of the latest ACT constraints).

Fortunately, there is a simple and natural solution to the problems with SIDR as a solution to the Hubble tension. The first problem can be avoided if SIDR is created after BBN. This is exactly what happens in the Hot New Early Dark Energy (Hot NEDE) model² [1, 30, 34, 35], where SIDR is created from the latent heat of a supercooled phase transition in the dark sector after BBN but before recombination [1, 30]. The second problem can be avoided if SIDR interacts with a fraction of dark matter early on, but decouples from dark matter just around equality in a process we refer to as dark radiation-matter decoupling (DRMD) [1]. In Hot NEDE, this is naturally achieved in a model where the phase transition is related to the spontaneous symmetry breaking of $SU(N) \rightarrow SU(N-1)$ [1]. In this setting, it has been shown that the Hubble tension can be reduced below 1.5σ when using Planck 2018 CMB, DESI DR2 BAO and Pantheon+ supernova data [1].

Other scenarios exhibit a similar decoupling feature. In the *Atomic Dark Matter* model, dark atoms form within the dark sector in a process analogous to recombination in the

² The general New Early Dark Energy (NEDE) framework for addressing the Hubble tension by a fast-triggered phase transition, and the general treatment of perturbations, with the possibility of the trigger field being either a scalar field, temperature, or something else, was first proposed in [32, 33].

visible sector [36–40]. In the *Stepped Partially Acoustic Dark Matter* model, decoupling instead occurs when a massive component of the dark radiation fluid annihilates away [41]. These scenarios have been explored as possible resolutions of the Hubble tension [42–44], and some achieve a comparable level of phenomenological success for the datasets mentioned above [45]. In their present form, they lack, however, a mechanism for creating dark radiation after BBN.

In the case of Hot NEDE, the decoupling mechanism was tested against data using an effective fluid description, which we refer to as the DRMD model [1]. It extends Λ CDM by three additional parameters: the amount of (self-interacting) dark radiation produced after BBN, parametrized by ΔN_{eff} ; the fraction of interacting dark matter, f_{idm} ; and the redshift of dark decoupling, z_{dec} . Both the previous results and those presented in this work therefore apply more broadly to scenarios in which a dark radiation component interacts with a fraction of dark matter and subsequently decouples around matter–radiation equality via an exponential suppression of the drag rate.

Just as decoupling creates a BAO feature in the matter power spectrum at a characteristic scale given by the sound-horizon when baryons decouple from the radiation bath of photons, in a similar way the dark matter and dark radiation interactions will, together with gravity, create acoustic oscillations in the dark fluid, and the DRMD process will create a Dark Acoustic Oscillation (DAO) at a characteristic scale set by the dark sound horizon at the time of dark decoupling [1, 2, 37, 46]. Thus the existence of a DAO at a characteristic scale, as well as its amplitude, is a prediction of this class of models and closely tied to their ability to resolve the Hubble tension. The aim of this work is to sharpen and quantify this connection between DAO and the Hubble tension.

In previous work [2], we showed that the existence of a DAO close in scale to the actual BAO, could bias the extraction of the BAO scale in the DESI analysis, if ignored. We furthermore showed that accounting for the DAO bias can explain the DESI DR2 anomaly as an alternative explanation to evolving dark energy. We also found that the DAO scale and amplitude, preferred by DESI compared to no DAO, matches the properties predicted by Hot NEDE with DRMD when resolving the Hubble tension, providing a first validation of DRMD as a solution to the Hubble tension [1].

The DAO predicted by DRMD can be further searched for in DESI full-shape data and future large-scale-structure surveys, such as Euclid [47], or the Roman Space Telescope [48].

To facilitate searches for the DAO predicted by DRMD-like solutions to the Hubble tension, we will here study the DAO predictions made by this class of solutions to the Hubble tension independently of large-scale structure observations like DESI. For this purpose we will extract the preferred scale and amplitude of the DAO when fitting the DRMD model to CMB and supernova data only. This prediction provides a target for current and future large-scale structure surveys. In particular we show that these predictions are consistent with results already extracted from the DESI DR2 data in [1], which, as discussed above, provides a preliminary validation of the importance of DRMD in resolving the Hubble tension.

The posterior distributions shown in Fig. 1 summarize the main results of this work. Starting from CMB data alone (black), we then add SH0ES-calibrated supernova data (purple dashed), and finally compare with a previous analysis in [1] that also included BAO data (blue dotted). The resulting constraints remain mutually consistent throughout. Moreover, they are also consistent with the DAO scale extracted independently of the DRMD model from DESI DR2 data, when taking into account how a DAO peak of a given scale would bias the extraction of the BAO scale [2].

This paper is organized as follows. In section II, we review the effective fluid model of DRMD, discuss why a decoupling feature is needed for solving the Hubble tension within this class of models, and explain the origin of the DAO feature in the DRMD model. In section III we discuss the results from our parameter inference, which includes targets for future full-shape analyses of the DESI data and future large-scale structure telescopes on ground or in space. We conclude with a discussion and outlook in section IV.

II. DARK RADIATION-MATTER DECOUPLING

The decoupling between dark radiation and dark matter within Hot NEDE is described by an effective fluid implementation, which we refer to as DRMD and which has also been implemented into the publicly available Boltzmann code `DRMD-CLASS`³ [1]. The DRMD mechanism and its implementation is however sufficiently general that the code can also be used to describe the phenomenology of certain other proposed scenarios falling within this class of models [41, 43]. For concreteness, we first briefly review the origin of a decoupling between dark radiation and dark matter in Hot NEDE, and comment on how our results

³ <https://github.com/NEDE-Cosmo/DRMD-CLASS.git>

apply more generally to other scenarios. After that, we proceed to describing the DRMD model in Sec. II A, before discussing the resolution of the Hubble tension in Sec. II B and DAO in Sec. II C.

In the Hot NEDE model of [1, 30], the dark sector is described by a weakly coupled $SU(N)$ gauge theory, including a light dark Higgs field Ψ and a heavy Dirac fermion dark matter multiplet χ , both of which transform under the fundamental representation of $SU(N)$, but are not coupled to the Standard Model sector. The Higgs field leads to spontaneous symmetry breaking from $SU(N)$ to $SU(N - 1)$ via a supercooled phase transition, taking place in the epoch after BBN but well before recombination. The associated latent heat creates a radiation plasma consisting of massless gauge bosons, A^a , of the unbroken $SU(N - 1)$ and the physical dark Higgs boson ψ , which arises when the complex scalar Ψ picks up a non-vanishing vacuum expectation value v , *i.e.* $|\Psi| \equiv (v + \psi)/\sqrt{2}$. The gauge interactions between the relativistic degrees of freedom lead to a tightly coupled fluid, which behaves like SIDR. Such a scenario is naturally realized for a Coleman-Weinberg potential with small explicit breaking of classical conformal invariance [49, 50]. This dark sector re-heating raises the effective number of relativistic degrees of freedom to⁴

$$\Delta N_{\text{eff}} \equiv \Delta N_{\text{NEDE}} \sim \left(\frac{g v}{85 \text{ keV}} \right)^4 \left(\frac{10^8}{1 + z_*} \right)^4 \quad (\text{for } N = 3), \quad (1)$$

where g is the $SU(N)$ gauge coupling and z_* denotes the redshift of the phase transition that must occur after BBN but before the first scales probed through the CMB start entering the horizon, implying $10^6 \lesssim z_* \lesssim 10^9$.

Before the phase transition a fraction f_{idm} of dark matter is in a multiplet, χ , charged under $SU(N)$ in the fundamental representation. After the phase transition, $N - 1$ components of the dark matter multiplet, χ_j , are charged under the unbroken $SU(N - 1)$ and interact with the dark radiation fluid, while the component in the broken direction χ_0 is neutral under the unbroken $SU(N - 1)$. Thus, χ_0 only interacts with the χ_j through dark matter scattering mediated by the massive gauge bosons with components along the broken directions $SU(N)/SU(N - 1)$, maintaining equilibrium between χ_j and χ_0 . Accordingly, after the phase transition, we can separate the fraction of interacting dark matter, f_{idm} , into a neutral, $f_{\chi_0}(z)$, and charged, $f_{\chi_j}(z)$, fraction: $f_{\text{idm}} = f_{\chi_j}(z) + f_{\chi_0}(z)$.

⁴ There is an additional small change to ΔN_{eff} when the Higgs boson becomes non-relativistic, but that is a sub-leading effect, which vanishes in the large- N limit, and so we ignore it here for simplicity. For a detailed discussion, see [30].

Initially after the phase transition, the fraction of interacting dark matter, f_{idm} , is in equilibrium with the dark radiation fluid through t -channel Compton scattering between the massless $SU(N-1)$ gauge bosons, A^a , and the charged dark matter component χ_j , while the χ_0 and χ_j , as mentioned above, maintain equilibrium with each other through t -channel dark matter scattering mediated by the massive gauge bosons along the broken directions. As a result, initially the χ particles and massless gauge bosons form a tightly coupled fluid similar to the photon-baryon fluid in the visible sector (for more details, see [1]).

Due to the fact that the χ_j and the χ_0 do not both couple to the massless gauge bosons A^a , their masses will receive different one-loop corrections after the symmetry breaking, leading to a small mass gap $\Delta m \approx g^3 v / (32\pi)$. Crucially, the neutral component χ_0 is lighter than its charged counterpart χ_j . This mass splitting is an unavoidable quantum effect. Therefore, as the temperature in the dark fluid, T_d , drops below the mass gap Δm , the charged dark matter component χ_j will become Boltzmann suppressed and convert into the neutral component χ_0 . The fraction $f_{\chi_j}(z)$ relative to f_{idm} can be therefore be written as

$$\left(\frac{f_{\chi_j}(z)}{f_{\text{idm}}}\right)_{\text{eq}} = \frac{(N-1)e^{-\Delta m/T_d}}{(N-1)e^{-\Delta m/T_d} + 1}. \quad (2)$$

Right after the phase transition, when $T_d \gg \Delta m$ the fractions satisfy equipartition

$$\left(\frac{f_{\chi_j}(z)}{f_{\text{idm}}}\right)_{\text{eq}} \rightarrow \frac{(N-1)}{N}, \quad (3)$$

but as the temperature later drops below the mass gap, $T_d < \Delta m$, the fraction of charged dark matter gets exponentially suppressed

$$\left(\frac{f_{\chi_j}(z)}{f_{\text{idm}}}\right)_{\text{eq}} \rightarrow (N-1)e^{-\Delta m/T_d}. \quad (4)$$

We denote the redshift at which the Boltzmann suppression becomes active at $T_d \approx \Delta m$ by z_{stop} . In other words, we parametrize

$$\exp\left(-\frac{\Delta m}{T_d}\right) = \exp\left(-\frac{1+z_{\text{stop}}}{1+z}\right). \quad (5)$$

Tight coupling between dark matter and dark radiation is maintained as long as the associated drag rate from t -channel Compton scattering within the $SU(N-1)$ gauge sector satisfies $\Gamma_{\text{drag}} \gg H$. The drag rate is given by

$$\Gamma_{\text{drag}} = \frac{f_{\chi_j}(z)}{f_{\text{idm}}} \Gamma_{\chi_j A_\mu^a}, \quad (6)$$

where $\Gamma_{\chi_j A_\mu^a}$ is the t -channel Compton interaction rate of χ_j states with the radiation bath of A^a bosons [1]. The ratio $\Gamma_{\chi_j A_\mu^a}/H$ is constant during radiation domination [24, 51], however, we infer that Γ_{drag}/H rapidly decreases once Boltzmann suppression kicks in for $z < z_{\text{stop}}$, and once the ratio drops below unity the dark radiation cannot maintain tight coupling to the non-relativistic χ -components, leading to the decoupling between dark matter and dark radiation. We denote the corresponding redshift when $\Gamma_{\text{drag}} = H$ by z_{dec} .

Before proceeding to discuss the effective fluid model of DRMD, let us pause to emphasize that the above discussion applies to any model or scenario where a fraction of dark matter, f_{idm} , transitions from being tightly coupled to self-interacting dark radiation to exponentially decoupling over the redshift interval $z_{\text{stop}} > z > z_{\text{dec}}$. Consequently, the DRMD fluid model described below, as well as the associated phenomenological results, are applicable to any scenario exhibiting this particular decoupling behavior, see *e.g.* [36–45, 52].

A. Effective Fluid Model of Dark Radiation-Matter Decoupling

At the fluid level, the perturbations in the dark sector are described by adding two new components, dark radiation and interacting dark matter (χ), to the standard Λ CDM model. As discussed above, due to the non-Abelian self-interactions of gauge bosons, the cosmological dynamics of the relativistic degrees of freedom can be described as a single fluid in terms of a density contrast δ_{DR} and a velocity divergence θ_{DR} . The initial energy density of the dark radiation fluid ρ_{DR} is parametrized in terms of its contribution to the effective number of neutrino species, ΔN_{eff} . Concretely, we define

$$\left(\frac{\rho_{\text{DR}}}{\rho_{1\nu}} \right)_{\text{ini}} = \Delta N_{\text{eff}}, \quad (7)$$

where $\rho_{1\nu} = \frac{7}{4} \frac{\pi^2}{30} (T_{\nu,0}/a)^4$ denotes the energy density of a single massless neutrino species with temperature $T_{\nu,0}$. In the context of Hot NEDE this ‘initial’ value is understood as the value *after* the supercooled phase transition that heats the dark sector, *i.e.* after BBN but before the modes observed in the CMB enter the horizon.

The non-relativistic, interacting dark matter component, with the neutral χ_0 and charged χ_j states assumed to be tightly coupled to each other, can be described by a pressureless fluid with density contrast δ_χ and velocity divergence θ_χ . The corresponding energy density

ρ_χ is measured relative to the total dark matter density

$$\rho_\chi = f_{\text{idm}}(\rho_{\text{cdm}} + \rho_\chi), \quad (8)$$

where ρ_{cdm} is the cold dark matter density. In synchronous gauge, the perturbation equations of the interacting dark matter component are

$$\delta'_\chi + \left(\theta_\chi + \frac{h'}{2} \right) = 0, \quad (9a)$$

$$\theta'_\chi + \mathcal{H}\theta_\chi = \mathcal{G}\Delta', \quad (9b)$$

where h is the trace of the spatial components of the metric fluctuation, and we introduced the velocity slip defined by $\Delta' = \theta_{\text{DR}} - \theta_\chi$. The time-dependent function \mathcal{G} quantifies the momentum-transfer between (interacting) dark matter and dark radiation and is determined by the drag-rate Γ_{drag} . Its time dependence can be parametrized through [1]

$$\mathcal{G} \simeq \mathcal{H} \left(\frac{\mathcal{G}}{\mathcal{H}} \right)_{\text{ini}} \left(1 + \frac{\Omega_m}{\Omega_{\text{rad}}} \frac{1}{1+z} \right)^{-1/2} \exp \left(-\frac{1+z_{\text{stop}}}{1+z} \right), \quad (10)$$

where for Hot NEDE the redshift-independent part can be related to the microphysical t -channel Compton interaction rate of the charged dark matter states (χ_j) with the radiation bath of the massless gauge bosons (A_μ^a)

$$\left[\frac{\mathcal{G}}{\mathcal{H}} \right]_{\text{ini}} = (N-1) \frac{a^2 \Gamma_{\chi_j A_\mu^a}}{a\mathcal{H}}, \quad (11)$$

where the right hand side is constant during radiation domination (after the Higgs has become non-relativistic and no longer contributes to the dark radiation fluid). The decoupling redshift z_{dec} is then defined through

$$\mathcal{G}(z_{\text{dec}}) = \mathcal{H}(z_{\text{dec}}). \quad (12)$$

Together with (10), it implies

$$\frac{1+z_{\text{stop}}}{1+z_{\text{dec}}} \simeq \ln \left(\left[\frac{\mathcal{G}}{\mathcal{H}} \right]_{\text{ini}} \right). \quad (13)$$

Similarly to the perturbation equations for the interacting dark matter component, the perturbation equations of the dark radiation fluid are [1]

$$\delta'_{\text{DR}} + (1+w_{\text{DR}}) \left(\theta_{\text{DR}} + \frac{h'}{2} \right) + 3\mathcal{H} (c_s^2 - w_{\text{DR}}) \delta_{\text{DR}} = 0, \quad (14a)$$

$$\theta'_{\text{DR}} - \frac{k^2 c_s^2}{1+w_{\text{DR}}} \delta_{\text{DR}} + \mathcal{H} (1-3c_s^2) \theta_{\text{DR}} = -\mathcal{G}R\Delta', \quad (14b)$$

with R follows from ensuring conservation of the combined dark matter-radiation fluid,

$$R = \frac{1}{1 + w_{\text{DR}}} \frac{\rho_{\chi}}{\rho_{\text{DR}}}, \quad (15)$$

and the sound speed in the radiation fluid

$$c_s^2 = w_{\text{DR}} - \frac{w'_{\text{DR}}}{3\mathcal{H}(1 + w_{\text{DR}})}. \quad (16)$$

We keep the equations general enough to allow for a time-dependence of the equation-of-state parameter w_{DR} . Since all the relevant scales are initially super-horizon, we can impose adiabatic super-horizon initial conditions (assuming that early enough $w_{\text{DR}} = 1/3$) [1]

$$\frac{4}{3}\delta_{\chi} = \delta_{\text{DR}} = \delta_{\gamma} = \delta_{\nu} = -\frac{2}{3}Ck^2\tau^2, \quad (17)$$

where C is an integration constant determined by matching to the co-moving curvature perturbation, while δ_{γ} is the photon and δ_{ν} the neutrino density contrast. At leading non-trivial order in $k\tau$, the perturbation equations imply the initial conditions for the dark radiation perturbations

$$\theta_{\text{DR}} = \theta_{\gamma} = -\frac{1}{18}Ck^4\tau^3, \quad (18)$$

and the dark matter velocity perturbations

$$\theta_{\chi} = \frac{(\mathcal{G}/\mathcal{H})_{\text{ini}}}{4 + (\mathcal{G}/\mathcal{H})_{\text{ini}}}\theta_{\gamma}. \quad (19)$$

DRMD-CLASS uses the dynamical equations in (9) and (14) supplemented by the initial conditions in (18) and (19). The redshift-dependence of the momentum transfer function \mathcal{G} is parametrized through (10). At the same time, z_{dec} as defined in (12) is inferred from the background evolution through linear interpolation on the integration grid.

B. The Hubble Tension

The angular size θ_s of the sound horizon in the CMB, which is very precisely determined by the position of the first peak, is given by the ratio of the comoving sound horizon $r_s(z_{LS})$ and the angular diameter distance $d_a(z_{LS})$ evaluated at the last scattering surface at $z = z_{LS}$. Since the Universe is matter dominated at the time of ordinary baryon-photon decoupling,

the angular diameter distance is approximately determined by the inverse Hubble rate today and Ω_m . Thus, one finds

$$\theta_s^{-1} = \frac{d_a(z_{LS})}{r_s(z_{LS})} \simeq \frac{1}{H_0 r_s} \int_0^{z_{LS}} dz [\Omega_m(1+z)^3 + (1-\Omega_m)]^{-1/2}. \quad (20)$$

As a result once $r_{d,\text{BAO}} \cdot H_0 \simeq r_s \cdot H_0$ is fixed by BAO measurements, Ω_m is determined by the relation between the angular size of the sound horizon measured in CMB and $r_{d,\text{BAO}} \cdot H_0$ measured by the BAO position independently of the precise value of H_0 itself.

However, since the relative matter density parameter Ω_m is fixed independent of H_0 , the physical matter density $\omega_m = \Omega_m h^2$, depends sensitively on the value of $H_0 \equiv h \, 100 \text{ km/s/Mpc}$. In particular, resolving the H_0 tension requires a larger than 10% increase in the physical matter density ω_m . Since the small-scale power in the CMB and the matter power spectrum depends on ω_m , models solving the Hubble tension tend to predict more power on small scales than predicted within ΛCDM . This effect is particularly severe for modes that enter *before* radiation-matter equality and are thus exposed to radiation-driving effects, which are sensitive to ω_m .

The DRMD mechanism is crucial for solving the Hubble tension, while not encountering this problem with too much power on small scales. In contrast, SIDR models (without an early coupling between dark matter and dark radiation) end up being limited in their ability to solve the Hubble tension by predicting too much power on small scales. A component of interacting dark matter will, due to its interactions with dark radiation, clump less than cold dark matter. It is dragged by dark radiation and effectively experiences a small positive pressure, suppressing the gravitational potential for any mode entering the horizon before it decouples at z_{dec} . For it to compensate the effect of a higher ω_m on only small scales entering before matter domination, but leave the large scales invariant, the interacting dark matter needs to decouple from dark radiation at around matter domination, *i.e.* $z_{\text{dec}} \sim z_{\text{eq}}$ [1]. This small-scale suppression is shown in the left panel of Fig. 2, which compares a typical DRMD temperature power spectrum (blue) to the corresponding SIDR spectrum with $f_{\text{idm}} = 0$ (red dashed). When this happens, DRMD allows for a full resolution of the Hubble tension when fitted to Planck 2018 CMB (and other data sets such as DESI DR2 BAO, and Pantheon+ supernova data [1]; see also left panel in Fig. 4). New data from ground based CMB experiments, such as ACT [31] and SPT [53], provide additional constraints on small scales. As we will discuss below, the imprint of the DAO in the CMB is however localized on

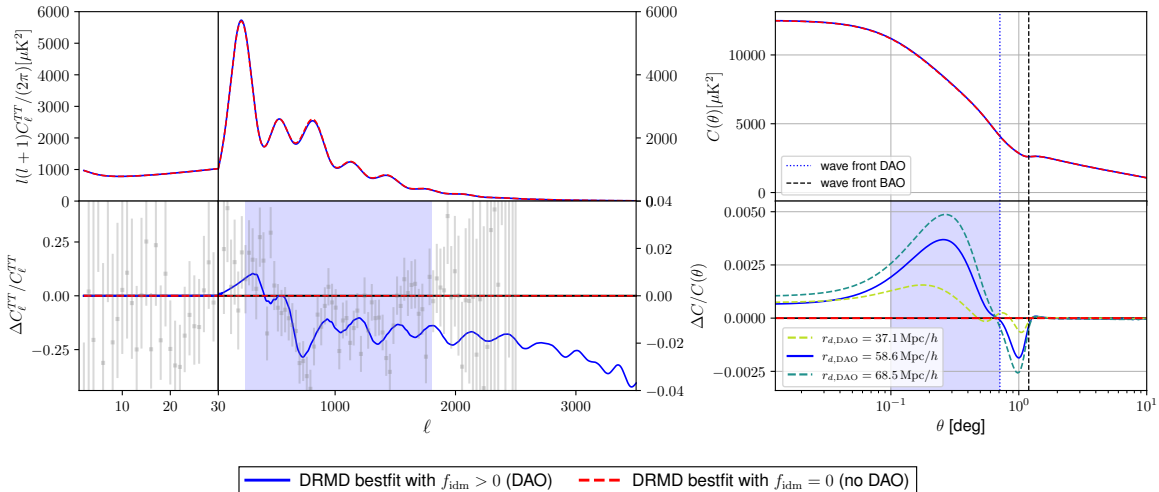


FIG. 2. CMB temperature anisotropies for the global best-fit obtained from our combined analysis with CMB and SH0ES-calibrated supernova data. We compare DRMD with DAO ($f_{\text{idm}} > 0$, blue) and without DAO ($f_{\text{idm}} = 0$, red dashed). The lower panels show the relative difference. *Left*: In harmonic space, the DAO imprint percent-level oscillatory features in the temperature power spectrum C_ℓ^{TT} , together with a broadband suppression induced by enhanced decay of the gravitational potential. Planck residuals are shown as gray error bars. We note the change in spacing of the axes as separated by the vertical line at $\ell = 30$. *Right*: In position space, this imprint appears as a localized feature in the angular correlation function $C(\theta)$ (blue-shaded band) at the permille level. The coloured dashed lines correspond to different choices of the DAO drag horizon scale.

intermediate scales best probed by Planck, and is therefore a robust prediction of the DRMD model's ability to address the Hubble tension (see also section IV).

C. Dark Acoustic Oscillations

Initially dark matter and dark radiation are tightly coupled. In this regime the two fluids share a common velocity divergence,

$$\theta_{\text{DR}} = \theta_\chi \equiv \theta, \quad (21)$$

which we denote as θ . Using Eqs. (9a) and (14a), and assuming adiabatic initial conditions at early times where $w_{\text{DR}} = 1/3$, we obtain

$$\frac{\delta_{\text{DR}}}{1 + w_{\text{DR}}} = \delta_\chi. \quad (22)$$

Furthermore, combining Eqs. (9b) and (14b) yields

$$\mathcal{G}\Delta' = 3c_{s,\text{eff}}^2 \left[\frac{k^2}{4}\delta_{\text{DR}} + \mathcal{H}\theta \right], \quad (23)$$

where we have defined

$$c_{s,\text{eff}}^2 = \frac{c_s^2}{1+R}. \quad (24)$$

It is convenient to introduce the total density perturbation

$$\delta\rho = \delta\rho_\chi + \delta\rho_{\text{DR}}, \quad \rho = \rho_\chi + \rho_{\text{DR}}, \quad (25)$$

and to rewrite the system in terms of the corresponding combined fluid variables $\delta = \delta\rho/\rho$ and θ . After straightforward algebra, the perturbation equations reduce to two independent equations,

$$\delta' + (1 + w_{\text{eff}}) \left(\theta + \frac{h'}{2} \right) + 3\mathcal{H} (c_{s,\text{eff}}^2 - w_{\text{eff}}) \delta = 0, \quad (26a)$$

$$\theta' - \frac{k^2 c_{s,\text{eff}}^2}{1 + w_{\text{eff}}} \delta + \mathcal{H} (1 - 3c_{s,\text{eff}}^2) \theta = 0. \quad (26b)$$

These are precisely the perturbation equations of a single fluid [54] with time-dependent equation-of-state parameter

$$w_{\text{eff}} = \frac{p_\chi + p_{\text{DR}}}{\rho_\chi + \rho_{\text{DR}}} = \frac{w_{\text{DR}}}{1 + (1 + w_{\text{DR}})R}. \quad (27)$$

In particular, using the definition in (24) alongside (15) and (16), we can indeed verify that $c_{s,\text{eff}}$ as defined in (24) agrees with the expression for the sound speed of a barotropic fluid

$$\frac{p'}{\rho'} = w_{\text{eff}} - \frac{w'_{\text{eff}}}{1 + 3\mathcal{H}(1 + w_{\text{eff}})} = c_{s,\text{eff}}^2. \quad (28)$$

This in turn allows us to define the dark acoustic (or dark drag) horizon,

$$r_{d,\text{DAO}} = \int_0^{\eta_{\text{dec}}} d\eta c_{s,\text{eff}}(\eta) = \int_{z_{\text{dec}}}^{\infty} dz \frac{c_{s,\text{eff}}(z)}{H(z)}, \quad (29)$$

which corresponds to the comoving distance a dark acoustic wave can travel prior to decoupling. As we will see below, this scale sets the characteristic angular size of DAO features in the CMB and in the matter distribution of the Universe.

To obtain an initial estimate, we note that the DRMD process is analogous to standard photon decoupling in the visible sector, although it occurs somewhat earlier, close to matter–radiation equality. In Λ CDM, the acoustic scale associated with baryon decoupling is

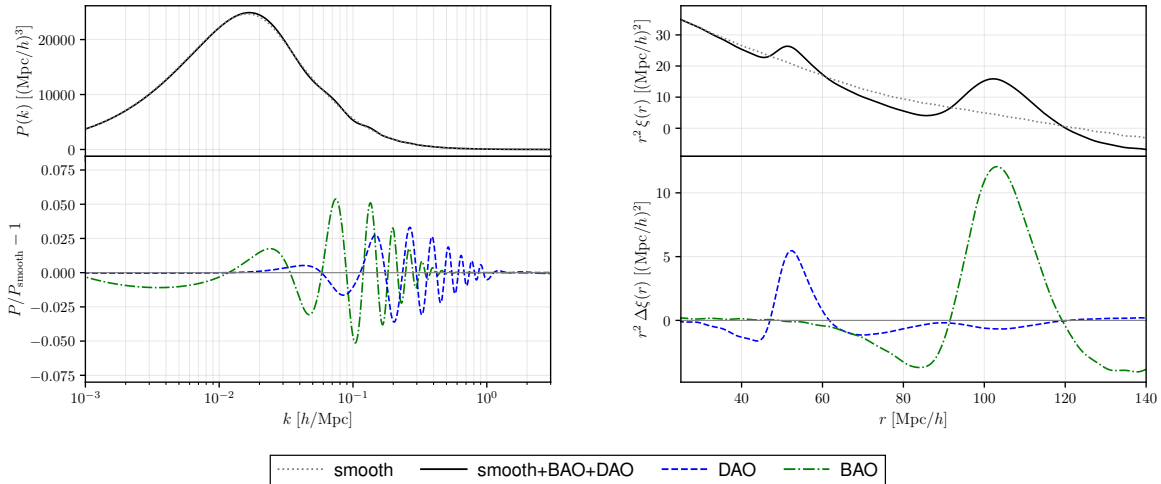


FIG. 3. BAO-DAO decomposition of the linear matter power spectrum $P_{\text{lin}}(k)$ (left) and corresponding correlation function $\xi(r)$ (right) for the global best-fit obtained from our combined analysis with CMB and SH0ES-calibrated supernova data. The lower panels show the DAO (blue) and BAO (green) features relative to the smooth broadband contribution (dotted lines in the upper panels). For details on the decomposition into smooth and wiggly BAO as well as DAO contributions, see section III.

$k_{A,\text{dec}} = \pi/r_{d,\text{BAO}} \approx 0.022 \text{ Mpc}^{-1}$, while the scale associated with matter–radiation equality is $k_{A,\text{eq}} = \pi/r_{d,\text{eq}} \approx 0.050 \text{ Mpc}^{-1}$, where the subscript A denotes the acoustic scale, which is half the full angular scale. The ratio of these two characteristic scales is therefore $k_{A,\text{dec}}/k_{A,\text{eq}} \approx 0.44$. Similar to the standard BAO feature at $r_{d,\text{BAO}} \approx 100 \text{ Mpc}/h$ (see Tab. I), one would then naively expect a DAO feature at roughly half that distance $r_{d,\text{DAO}} \approx 50 \text{ Mpc}/h$. In Fig. 3, we extract the BAO and DAO contributions from the best-fit DRMD model to the linear matter power spectrum $P_{\text{lin}}(k)$ as well as the corresponding correlation function $\xi(r)$, and indeed find the DAO feature located close to $r_{d,\text{DAO}} \approx 50 \text{ Mpc}/h$, in agreement with this simple estimate.

Before returning to the properties of these DAO features and their impact on matter clustering in more detail, let us stress that their effect on the CMB angular power spectrum is much smaller. This is because the DM-DR interaction directly influences the matter perturbations, while the impact on photons is only indirect via the associated metric perturbations. More precisely, the relative size of DAO versus BAO features in the matter distribution is controlled by the ratio of densities of interacting dark matter and baryons, *i.e.* f_{idm}/f_b where f_b is the baryon fraction. On the other hand, for the CMB, the acoustic peaks driven by sound waves of the photon-baryon plasma are an $\mathcal{O}(1)$ effect, while the

impact of DAO is transmitted only via their impact on gravitational potentials, which is suppressed as $(\rho_{\text{idm}} + \rho_{\text{DR}})/\rho_{\text{tot}}$. This ratio is of order $0.13 \Delta N_{\text{eff}}$ before equality and goes to f_{idm} thereafter.

For the CMB (neglecting the difference between the the sound horizon at baryon decoupling and at last scattering) these scales subtend angles $\theta_{A,\text{dec}} = r_{d,\text{BAO}}/d_A(z_{LS}) \approx 0.01 \text{ rad} \approx 0.6^\circ$, $\theta_{\text{eq}} = r_{d,\text{eq}}/d_A(z_{LS}) \approx 0.005 \text{ rad} \approx 0.3^\circ$, where we have used $d_A(z_{LS}) = 13.9 \text{ Gpc}$ for the angular diameter distance. These angular scales can be identified directly in position space via the angular correlation function

$$C(\theta) = \sum_{\ell} \frac{2\ell + 1}{4\pi} C_{\ell} P_{\ell}(\cos \theta), \quad (30)$$

shown in the right panels of Fig. 2. In particular, the estimate $\theta_{\text{eq}} \approx 0.3^\circ$ corresponds to the bump visible in the lower-right panel of Fig. 2, where the blue line denotes the DRMD best-fit cosmology. This feature extends over a finite range of angular scales (indicated by the blue-shaded region) that is especially well probed by Planck 2018 (see residuals in lower left panel). For comparison, we also display models with smaller and larger drag horizons (dashed lines), which shift the feature to correspondingly smaller and larger angles.

The small dip at slightly larger scales arises from the broadband modification induced by the dark matter–dark radiation interaction, which affects the BAO. The acoustic interpretation of both the peak and dip becomes even clearer when displaying the wave fronts, which represent the causal propagation limit and are expected at twice the corresponding horizon scale [55]. In our case, they occur at angular scales $2r_{d,\text{DAO}}/d_A(z_{LS}) \approx 0.6^\circ$ (blue dotted) for the DAO and at $2r_{d,\text{BAO}}/d_A(z_{LS}) \approx 1.2^\circ$ (black dotted) for the BAO feature, thereby delineating the angular extent of both features.⁵

In multipole space, these two acoustic/sound horizon scales correspond approximately to $\ell_{A,\text{dec}} \sim 300$ and $\ell_{\text{eq}} \sim 600$, which roughly correspond (up to a phase shift) to the first standard acoustic peak and to the pronounced dip within the blue-shaded band associated with the DAO position-space feature. The broadband effect, on the other hand, is visible as the overall suppression of power compared to the SIDR reference cosmology (with $f_{\text{idm}} = 0$). As discussed in more detail in [1], it arises because the radiation pressure exerted on dark

⁵ As discussed in detail in [55], the BAO feature does not manifest itself as a peak in the angular correlation function $C(\theta)$. Instead, its wave front can be identified as an edge feature similar to the one in the upper right panel.

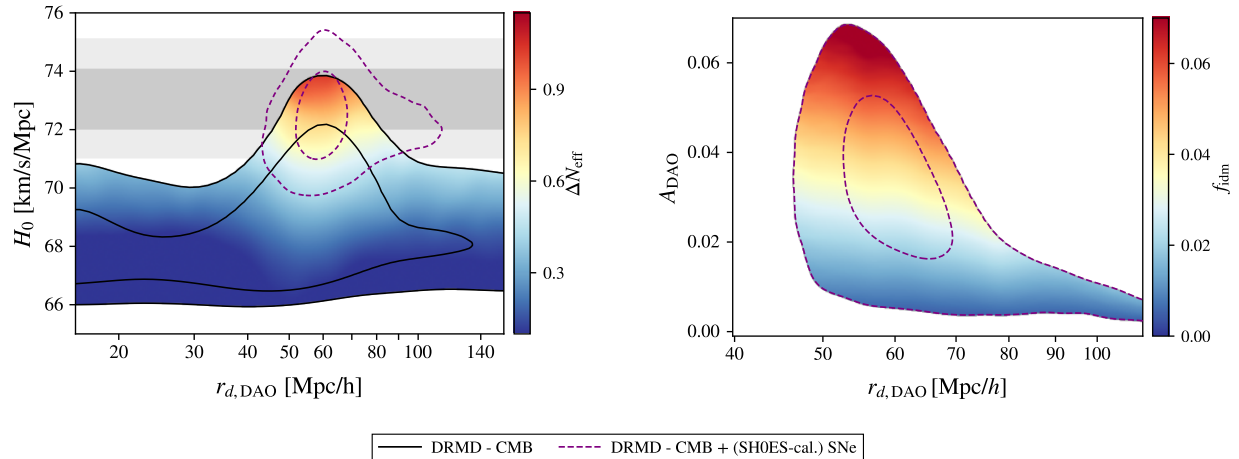


FIG. 4. Marginalized 2D posterior from our analysis using CMB data (black) and CMB combined with calibrated supernova (purple dashed). The inner and outer contours correspond to the 68% and 95% confidence levels. *Left:* The SH0ES determination of H_0 is shown as the gray band [3]. Within DRMD, Planck 2018 becomes fully consistent with SH0ES. Marginalization over $r_{d,DAO}$ induces strong projection effects due to parameter degeneracies, which are largely broken by including calibrated supernova data. *Right:* Targets for future searches: DRMD predicts a percent-level DAO amplitude at dark drag horizon scales of approximately 60 Mpc/h.

matter leads to an excess decay of the gravitational potential (off-setting the effect of an increased ω_m). A feature at 0.6° ($l \approx 600$) is well within the Planck regime, and not in the regime where ground based experiments like ACT and SPT are expected to improve the constraints. For more discussion of this aspect, see also section IV.

These numerical values should be regarded as order-of-magnitude estimates. A precise characterization of the DAO requires the full Boltzmann analysis presented in the next section.

III. PARAMETER CONSTRAINTS AND DAO TARGETS

To obtain a quantitative prediction for the DAO feature, we perform a cosmological parameter inference using the publicly available DRMD-CLASS code [1], which is based on the Cosmic Linear Anisotropy Solving System CLASS [56]. We consider an extension of Λ CDM that introduces three additional parameters: the amount of self-interacting dark radiation ΔN_{eff} (defined in (7)), the fraction of interacting dark matter f_{idm} (defined in (8)), and the

redshift z_{stop} at which the exponential suppression of the drag rate sets in (defined in (5)).

The decoupling redshift z_{dec} is treated as a derived parameter using Eq. (12). Likewise, the DAO drag horizon $r_{d,\text{DAO}}$ is derived from Eq. (29). The initial interaction strength is fixed to an arbitrary value corresponding to initial tight coupling, $(\mathcal{G}/\mathcal{H})_{\text{ini}} = 10^7$. As discussed in [1] (see also Eq. (13)), for a given z_{dec} this parameter is degenerate with z_{stop} , and including it in the sampling would just introduce a flat direction. In the current implementation we set $w_{\text{DR}} = c_s^2 = 1/3$, neglecting mass-threshold effects, and assume a mechanism such as Hot NEDE to generate a sizeable ΔN_{eff} after BBN [30]. We accordingly use the Helium abundance prediction from BBN that applies for a Λ CDM cosmology with $\Delta N_{\text{eff}} = 0$.

For the parameter inference we use the general-purpose Bayesian analysis framework Cobaya [57]. We impose flat priors

$$\Delta N_{\text{eff}} \in [0, 3], \quad f_{\text{idm}} \in [0, 1], \quad \log_{10}(z_{\text{stop}}) \in [3, 5.3], \quad (31)$$

while adopting standard priors for the six Λ CDM parameters. We further assume one massive neutrino with $m_3 = 0.06$ eV and temperature $T_3 = 0.716 T_\gamma$.

We perform two Metropolis-Hastings Markov Chain Monte Carlo (MCMC) analyses. The baseline run (performed for Λ CDM and DRMD) includes Planck 2018 CMB anisotropy measurements [4, 58], incorporating high- ℓ TT+TE+EE spectra, low- ℓ TT+EE spectra, and CMB lensing. The extended run additionally includes the Pantheon+ supernova sample [11], calibrated using the SH0ES prior on the absolute magnitude M [3] (amounting to $H_0 = 73.04 \pm 1.04$ km/s/Mpc for late-time Λ CDM cosmologies). We quantify the residual Hubble tension using the posterior distribution of the difference $\Delta \equiv H_0^{\text{CMB}} - H_0^{\text{SH0ES}}$, obtained by convolving the marginalized one-dimensional posteriors of the two measurements (SH0ES and CMB only). The two-sided posterior tail probability for $\Delta = 0$ is then converted into an equivalent Gaussian significance, which we quote as the residual tension in units of σ .

This setup follows a two-step logic. The baseline run demonstrates that DRMD reconciles Planck and SH0ES measurements. The extended run, which provides tighter parameter constraints, is then used to infer and predict the properties of the DAO feature.

The MCMC results are summarized in Tab. I and Fig. 4. The baseline DRMD run reduces the Hubble tension to the 2σ level, despite being affected by strong projection effects. This is evident in the left panel of Fig. 4, which shows a clear overlap of the 95% credible regions between the SH0ES band (gray) and the DRMD posterior (color-coded). Importantly, this

overlap only occurs for dark drag-horizon scales in the range $40 \text{ Mpc}/h < r_{d,\text{DAO}} < 80 \text{ Mpc}/h$. Outside this interval, the two datasets become clearly incompatible. This demonstrates that the presence of the DAO feature is essential for making the CMB compatible with large values of ΔN_{eff} and thus resolving the Hubble tension within the DRMD model.

At the same time, marginalizing over $r_{d,\text{DAO}}$ (or equivalently over $\log_{10}(z_{\text{stop}})$) induces a pronounced projection effect (commonly encountered in extensions of ΛCDM [59–61]). This results in an apparently low marginalized value, $H_0 = 68.7_{-1.8}^{+0.9} \text{ km/s/Mpc}$. In principle, a profile-likelihood analysis can mitigate such projection effects. Indeed, for a closely related dataset combination, Ref. [1] reported a residual 1.4σ tension using the *difference of the maximum a posteriori* (DMAP) estimator. Here, however, we restrict ourselves to the Bayesian analysis, which, using the method described above, results in a mild residual tension of 2.3σ despite the presence of strong projection effects. This is then further supported by the 2D posterior shown in Fig. 4, which similarly demonstrates that DRMD renders the two datasets statistically compatible.

As expected, including the SH0ES-calibrated supernova data selects the region of parameter space in which the DAO horizon scale lies within the previously identified narrow interval and ΔN_{eff} takes on sizeable values (purple dashed contour).

For this dataset combination, we perform a more detailed characterization of the DAO signal beyond its horizon scale in a dedicated post-processing step. To be specific, we decompose the linear matter power spectrum as

$$P_{\text{lin}}(k) = P_{\text{smooth}}(k) + P_{\text{BAO}}(k) + P_{\text{DAO}}(k). \quad (32)$$

An example of this decomposition is shown in Fig. 3, where the BAO and DAO contributions are displayed as the green dash-dotted and blue dashed curves, respectively. The decomposition is obtained by performing, for each DRMD cosmology, a corresponding SIDR reference run with identical background evolution but no interactions between dark matter and dark radiation. In practice, this is implemented by setting $f_{\text{idm}} = 0$ while keeping the total dark matter abundance fixed. We then apply a smooth–wiggly split to both cosmologies using a Gaussian smoothing kernel, supplemented by a low-order polynomial correction to ensure an accurate broadband fit.⁶ For the DRMD cosmology, the oscillatory component contains

⁶ In practice, we apply a Gaussian smoothing in $\ln k$ with $\Delta \ln k = 0.25$, plus a cubic $\ln k$ polynomial correction fit to $\ln(P/P_{\text{smooth}})$ over $k \in [0.001, 5.5] h \text{ Mpc}^{-1}$.

both BAO and DAO contributions, whereas for the SIDR reference model it contains only BAO. This procedure therefore allows us to isolate and disentangle the DAO signal from the standard BAO feature.

The validity of this procedure is most directly assessed in position space. To this end, we consider the two-point correlation function,

$$\xi(r) = \frac{1}{2\pi^2} \int_0^\infty dk k^2 P_{\text{lin}}(k) \frac{\sin(kr)}{kr}, \quad (33)$$

which directly relates oscillatory features in $P_{\text{lin}}(k)$ to localized structures in real space. Applying this transform separately to P_{BAO} and P_{DAO} for our best-fit DRMD cosmology yields distinct peaks at $r \approx 100 \text{ Mpc}/h$ and $r \approx 60 \text{ Mpc}/h$, respectively, as shown in the lower-right panel of Fig. 3. Importantly, the peaks do not exhibit noticeable leakage: the BAO component does not generate a spurious feature at the DAO scale, and vice versa. This clean separation in configuration space confirms the robustness of our decomposition procedure.

This analysis allows us to quantify the amplitudes of the oscillatory features. We define

$$A_{\text{DAO}} = \max\left(\frac{|P_{\text{DAO}}|}{P_{\text{smooth}}}\right), \quad A_{\text{BAO}} = \max\left(\frac{|P_{\text{BAO}}|}{P_{\text{smooth}}}\right), \quad (34)$$

where the maxima are taken over $k \in [0.01, 2] h \text{ Mpc}^{-1}$.

This procedure admits a quantitative prediction of the DAO feature in terms of its drag horizon and amplitude. As the main result of this work, we obtain

$$r_{d,\text{DAO}} \in [53.7, 64.8] \text{ Mpc}/h, \quad A_{\text{DAO}} = 0.031^{+0.014}_{-0.011} \quad (68\% \text{ C.I.}). \quad (35)$$

These predictions for the properties of a DAO feature in the matter power spectrum obtained from the resolution of the Hubble tension within the DRMD model based on only Planck CMB and (SH0ES-calibrated) supernova data are illustrated by the 2D posterior contours in the right panel of Fig. 4 and can be used for a targeted feature search in large-scale structure data. As a simple consistency check, the color-coding in Fig. 4 indicates that larger values of A_{DAO} correspond to larger values of f_{idm} , as expected. For comparison, the considerably tighter BAO constraints read

$$r_{d,\text{BAO}} = 100.1 \pm 1.1 \text{ Mpc}/h, \quad A_{\text{BAO}} = 0.0531^{+0.0013}_{-0.0015} \quad (68\% \text{ C.I.}). \quad (36)$$

In other words, the DAO amplitude can be substantially smaller than its BAO counterpart. However, if the model is to play a significant role in addressing the Hubble tension, A_{DAO} should not fall far below the percent level.

In Fig. 1, we display the one-dimensional posterior for the drag horizon $r_{d,\text{DAO}}$ (purple dashed) and compare it with results from earlier analyses. We find excellent agreement with the constraints reported in Ref. [1] (blue dotted), which considered a four-parameter version of the DRMD model (featuring an additional degeneracy direction associated with $(\mathcal{G}/\mathcal{H})_{\text{ini}}$) and included DESI DR2 BAO data.⁷ Remarkably, our result is also compatible with the “negative branch” identified in the DAO bias analysis of Ref. [2] in the context of the DESI anomaly. We stress that the present determination constitutes an entirely independent inference of the DAO signal. Thus the match of the CMB/SH0ES preference for a DAO scale of order $60 \text{ Mpc}/h$ related to resolving the Hubble tension and the independent DESI DR2 preference related to the DESI anomaly constitutes a non-trivial concordance within DRMD.

Overall, if the Hubble tension is resolved through new decoupling physics as captured by the DRMD model, the above values constitute a falsifiable signature of this scenario that can be looked for in current and future large-scale structure surveys.

IV. DISCUSSION AND OUTLOOK

Both the Hubble tension and the DESI anomaly challenge the ΛCDM model as a complete description of our Universe. Among them, the Hubble tension, a discrepancy between the value of H_0 inferred from CMB fits within ΛCDM and the locally measured value from supernova observations, currently provides the most statistically significant evidence for physics beyond ΛCDM .

The DRMD model is a three-parameter extension of ΛCDM , featuring a component of interacting dark matter, which decouples from a component of self-interacting dark radiation around matter-radiation equality. We have shown that DRMD can resolve the Hubble tension when fitted only to Planck 2018 CMB data. In this case, the Hubble tension is reduced to 2.3σ , compared to more than 5σ in ΛCDM . Crucially, a decoupling of interacting dark matter and self-interacting dark radiation around matter-radiation equality predicts the existence of DAO on an acoustic scale of roughly half the BAO scale. The regime of DRMD fitted to Planck 2018 data, which reduces the Hubble tension below 3σ shows a clear

⁷ The one-dimensional posterior shown here was obtained by post-processing the MCMC chains of Ref. [1] to include $r_{d,\text{DAO}}$ as a derived parameter using Eq. (29).

preference for a DAO with these features.

Once we complement the data analysis with SH0ES-calibrated supernova data, this preference sharpens into the prediction quoted in (35), independently of large-scale structure surveys such as DESI. We note that the posterior for $r_{d,\text{DAO}}$ is markedly non-Gaussian and extends to large values of $r_{d,\text{DAO}}$, including values exceeding $r_{d,\text{BAO}}$, always at non-zero A_{DAO} .

Independently of DRMD and the Hubble tension, in previous work [2] we investigated whether the anomaly in the DESI DR2 data, typically interpreted in terms of evolving dark energy, can instead be explained by the presence of a DAO peak which biases the determination of the BAO peak position. We showed that DAO can indeed explain the anomaly and are preferred over the null hypothesis of no DAO with more than five units of χ^2 , with a preferred position and amplitude closely overlapping with the DAO properties found in this work (independently of DESI and other large-scale structure data using only CMB and supernova data). The presence of DAO provides an arguably more convincing interpretation of the DESI DR2 data than evolving dark energy, the interpretation preferred by the DESI collaboration itself, as evolving dark energy cannot obviously be related to the Hubble tension. From an Occam's razor standpoint, we therefore believe the DAO interpretation of the DESI anomaly, which connects both problems, is a more credible explanation.

The predictions of the position and amplitude of the DAO obtained from fitting DRMD to the CMB and (SH0ES-calibrated) supernova data, independent of BAO and large-scale structure data, provides a target for present and future large-scale structure surveys like DESI [62], Euclid [47], and the Roman Space Telescope [48]. The evidence for the DAO from the bias analysis of the DESI DR2 data provides a first preliminary and independent validation from large-scale structure surveys. Future full-shape analyses of the DESI data as well as large-scale structure data will be able to constrain more decisively whether DAO arising within the DRMD model provide an explanation of the Hubble tension and the DESI anomaly.

The DAO feature predicted by the DRMD model in the matter power spectrum leaves only a much weaker imprint in the CMB angular power spectrum, since the DM-DR interaction directly impacts matter perturbations but only indirectly affects CMB photons. Nevertheless, as is well-known, the extra relativistic dark fluid component also leads to a broadband effect on the CMB on small angular scales. Therefore, another important constraint on DRMD comes from new CMB observations extending to smaller scales and yield-

ing higher quality polarization data than Planck, such as ACT [31] or SPT [53]. The latest results from ACT and SPT are painting a complicated picture. While the ACT constraints on (free-streaming) ΔN_{eff} are tighter than the constraints from Planck, the SPT constraints on ΔN_{eff} are more loose. The stronger ACT constraints arise because ACT observes more power on small scales in the CMB, which is contrary to the extra radiation-damping one would observe with a sizeable $\Delta N_{\text{eff}} \gtrsim 0.5$ as predicted in DRMD. One could object that DRMD relies on self-interacting (rather than free-streaming) radiation and features additional interactions with dark matter not present in simple $\Lambda\text{CDM} + N_{\text{eff}}$ cosmologies, but first results in the literature indicate that this is still not sufficient to reach large enough values of H_0 [63] to resolve the Hubble tension. Therefore, if the DRMD model is the correct solution to the Hubble tension, there are two possible explanations of the ACT data. One possibility is a residual foreground effect in ACT data, as the scales where ACT observes extra power is exactly the scales where foreground effects quickly become sizeable, diminishing the signal-to-noise ratio. While the ACT collaboration has made significant and impressive efforts to ensure that residual foreground effects are not driving their stronger constraints, this possibility needs yet to be tested further. Another possibility is to mildly extend the cosmological model to make it consistent with ACT data, while still resolving the Hubble tension [64]. We have shown that the DAO feature is a localized feature in real angular space located at approximately 0.3° , which corresponds to around $l \approx 600$ in multipole space, which is well within the Planck regime. We therefore do not expect that any mild parameter extensions addressing the issue with ACT data on small scales will affect the DAO prediction. The predictions presented here can thus be considered as a robust prediction of any model, within the DRMD class of models, solving the Hubble tension and agreeing with CMB observations on angular scales dominated by Planck, while potentially allowing for additional physics affecting only the broadband shape on very small angular scales.

Acknowledgements

We acknowledge Shi-Fan (Stephen) Chen, Ricardo Z. Ferreira, Laura Herold, Mikhail Ivanov, and Benjamin Wallisch for useful conversations. MG acknowledges support by the Excellence Cluster ORIGINS, which is funded by the Deutsche Forschungsgemeinschaft (DFG, German Research Foundation) under Germany’s Excellence Strategy – EXC-2094 - 390783311 as well as the DFG Collaborative Research Centre “Neutrinos and Dark Matter in Astro- and Particle Physics” (SFB 1258). FN was supported by VR Starting Grant 2022-03160 of the Swedish Research Council. MSS acknowledges Nordita for their kind hospitality through the Nordita corresponding fellow program.

	Λ CDM	DRMD	DRMD + (SH0ES-cal.) SN
Parameter	68% limits (best-fit)	68% limits (best-fit)	68% limits (best-fit)
ω_b	0.02236 ± 0.00015 (0.02240)	$0.02250^{+0.00018}_{-0.00027}$ (0.02255)	0.02311 ± 0.00018 (0.02318)
ω_{cdm}	0.1199 ± 0.0012 (0.1198)	$0.1241^{+0.0019}_{-0.0053}$ (0.1258)	0.1375 ± 0.0046 (0.1382)
H_0 [km/s/Mpc]	67.36 ± 0.54 (67.43)	$68.32^{+0.71}_{-1.7}$ (68.23)	72.40 ± 0.91 (72.50)
$\ln(10^{10} A_s)$	3.044 ± 0.015 (3.047)	3.045 ± 0.015 (3.042)	3.047 ± 0.015 (3.051)
n_s	0.9646 ± 0.0041 (0.9659)	$0.9674^{+0.0047}_{-0.0062}$ (0.9688)	0.9778 ± 0.0048 (0.9798)
τ_{reio}	0.0541 ± 0.0076 (0.0564)	0.0543 ± 0.0075 (0.0507)	0.0574 ± 0.0075 (0.0581)
ΔN_{eff}	–	< 0.590 (0.217)	0.85 ± 0.17 (0.87)
$\log_{10}(z_{\text{dec}})$	–	$3.32^{+0.77}_{-0.16}$ (3.34)	$3.316^{+0.075}_{-0.024}$ (3.350)
f_{idm}	–	< 0.702 (0.020)	$0.035^{+0.015}_{-0.013}$ (0.039)
Ω_m	0.3151 ± 0.0074 (0.3127)	0.3156 ± 0.0093 (0.3185)	0.3076 ± 0.0082 (0.3070)
$r_{d,\text{BAO}}$ [Mpc/h]	99.11 ± 0.93	99.1 ± 1.2 (98.5)	100.1 ± 1.1 (100.0)
$r_{d,\text{DAO}}$ [Mpc/h]	–	57^{+9}_{-60} (55.154)	[53.7, 64.8] (58.6)
$(r_{d,\text{DAO}} - r_{d,\text{BAO}})/r_{d,\text{BAO}}$	–	–	[–0.460, –0.352]
A_{DAO}	–	–	$0.031^{+0.014}_{-0.011}$ (0.036)
A_{BAO}	–	–	$0.0531^{+0.0013}_{-0.0015}$ (0.0538)
$\tilde{A} = A_{\text{DAO}}/A_{\text{BAO}}$	–	–	$0.59^{+0.25}_{-0.20}$ (0.67)
H_0 tension (Bayesian)	5σ	2.3σ	–
$\Delta\chi^2$ (rel. to Λ CDM)	0	–1.9	–31.7

TABLE I. Posterior means and 68% credible intervals for parameters inferred from the baseline analysis under Λ CDM and DRMD (left and middle columns), and from the extended analysis including calibrated supernova (SN) data (right column). One-sided constraints are quoted at 95% confidence. In cases where the posterior mean lies outside the 68% credible interval due to extended one-sided tails, we report only the credible interval (centred on the median).

-
- [1] M. Garny, F. Niedermann, H. Rubira, and M. S. Sloth, Hot New Early Dark Energy: Dark Radiation Matter Decoupling (2025), arXiv:2508.03795 [astro-ph.CO].
- [2] M. Garny, F. Niedermann, and M. S. Sloth, Dark Acoustic Oscillations as an Early-Universe Explanation of the DESI Anomaly (2025), arXiv:2512.15870 [astro-ph.CO].
- [3] A. G. Riess *et al.*, A Comprehensive Measurement of the Local Value of the Hubble Constant with $1 \text{ km s}^{-1} \text{ Mpc}^{-1}$ Uncertainty from the Hubble Space Telescope and the SH0ES Team, *Astrophys. J. Lett.* **934**, L7 (2022), arXiv:2112.04510 [astro-ph.CO].
- [4] N. Aghanim *et al.* (Planck), Planck 2018 results. VI. Cosmological parameters, *Astron. Astrophys.* **641**, A6 (2020), [Erratum: *Astron. Astrophys.* 652, C4 (2021)], arXiv:1807.06209 [astro-ph.CO].
- [5] S. Casertano *et al.* (H0DN), The Local Distance Network: a community consensus report on the measurement of the Hubble constant at 1% precision (2025), arXiv:2510.23823 [astro-ph.CO].
- [6] M. Abdul Karim *et al.* (DESI), DESI DR2 results. II. Measurements of baryon acoustic oscillations and cosmological constraints, *Phys. Rev. D* **112**, 083515 (2025), arXiv:2503.14738 [astro-ph.CO].
- [7] N. Schöneberg, G. Franco Abellán, A. Pérez Sánchez, S. J. Witte, V. Poulin, and J. Lesgourgues, The H0 Olympics: A fair ranking of proposed models, *Phys. Rept.* **984**, 1 (2022), arXiv:2107.10291 [astro-ph.CO].
- [8] E. Abdalla *et al.*, Cosmology intertwined: A review of the particle physics, astrophysics, and cosmology associated with the cosmological tensions and anomalies, *JHEAp* **34**, 49 (2022), arXiv:2203.06142 [astro-ph.CO].
- [9] E. Di Valentino *et al.* (CosmoVerse Network), The CosmoVerse White Paper: Addressing observational tensions in cosmology with systematics and fundamental physics, *Phys. Dark Univ.* **49**, 101965 (2025), arXiv:2504.01669 [astro-ph.CO].
- [10] D. Scolnic *et al.*, The Pantheon+ Analysis: The Full Data Set and Light-curve Release, *Astrophys. J.* **938**, 113 (2022), arXiv:2112.03863 [astro-ph.CO].
- [11] D. Brout *et al.*, The Pantheon+ Analysis: Cosmological Constraints, *Astrophys. J.* **938**, 110 (2022), arXiv:2202.04077 [astro-ph.CO].

- [12] J. Khoury, M.-X. Lin, and M. Trodden, Apparent $w < -1$ and a Lower S8 from Dark Axion and Dark Baryons Interactions, *Phys. Rev. Lett.* **135**, 181001 (2025), arXiv:2503.16415 [astro-ph.CO].
- [13] R. Kou and A. Lewis, Unified dark fluid with null sound speed as an alternative to phantom dark energy (2025), arXiv:2509.16155 [astro-ph.CO].
- [14] R. Chen, J. M. Cline, V. Muralidharan, and B. Salewicz, Quintessential dark energy crossing the phantom divide (2025), arXiv:2508.19101 [astro-ph.CO].
- [15] R. Liu, Y. Zhu, W. Hu, and V. Miranda, Phantom Mirage from Axion Dark Energy (2025), arXiv:2510.14957 [astro-ph.CO].
- [16] J.-Q. Wang, R.-G. Cai, Z.-K. Guo, and S.-J. Wang, Resolving the Planck-DESI tension by non-minimally coupled quintessence (2025), arXiv:2508.01759 [astro-ph.CO].
- [17] R. R. Caldwell and E. V. Linder, Null Impact of the Null Energy Condition in Current Cosmology (2025), arXiv:2511.07526 [astro-ph.CO].
- [18] S. Sánchez López, A. Karam, and D. K. Hazra, Non-Minimally Coupled Quintessence in Light of DESI (2025), arXiv:2510.14941 [astro-ph.CO].
- [19] A. Bedroya, G. Obied, C. Vafa, and D. H. Wu, Evolving Dark Sector and the Dark Dimension Scenario (2025), arXiv:2507.03090 [astro-ph.CO].
- [20] J. L. Bernal, L. Verde, and A. G. Riess, The trouble with H_0 , *JCAP* **10**, 019, arXiv:1607.05617 [astro-ph.CO].
- [21] L. Knox and M. Millea, Hubble constant hunter’s guide, *Phys. Rev. D* **101**, 043533 (2020), arXiv:1908.03663 [astro-ph.CO].
- [22] Z. Hou, R. Keisler, L. Knox, M. Millea, and C. Reichardt, How Massless Neutrinos Affect the Cosmic Microwave Background Damping Tail, *Phys. Rev. D* **87**, 083008 (2013), arXiv:1104.2333 [astro-ph.CO].
- [23] K. S. Jeong and F. Takahashi, Self-interacting Dark Radiation, *Phys. Lett. B* **725**, 134 (2013), arXiv:1305.6521 [hep-ph].
- [24] M. A. Buen-Abad, G. Marques-Tavares, and M. Schmaltz, Non-Abelian dark matter and dark radiation, *Phys. Rev. D* **92**, 023531 (2015), arXiv:1505.03542 [hep-ph].
- [25] M. A. Buen-Abad, M. Schmaltz, J. Lesgourgues, and T. Brinckmann, Interacting Dark Sector and Precision Cosmology, *JCAP* **01**, 008, arXiv:1708.09406 [astro-ph.CO].

- [26] M. Archidiacono, S. Gariazzo, C. Giunti, S. Hannestad, and T. Tram, Sterile neutrino self-interactions: H_0 tension and short-baseline anomalies, *JCAP* **12**, 029, arXiv:2006.12885 [astro-ph.CO].
- [27] N. Blinov and G. Marques-Tavares, Interacting radiation after Planck and its implications for the Hubble Tension, *JCAP* **09**, 029, arXiv:2003.08387 [astro-ph.CO].
- [28] D. Aloni, A. Berlin, M. Joseph, M. Schmaltz, and N. Weiner, A Step in understanding the Hubble tension, *Phys. Rev. D* **105**, 123516 (2022), arXiv:2111.00014 [astro-ph.CO].
- [29] N. Schöneberg and G. Franco Abellán, A step in the right direction? Analyzing the Wess Zumino Dark Radiation solution to the Hubble tension, *JCAP* **12**, 001, arXiv:2206.11276 [astro-ph.CO].
- [30] M. Garny, F. Niedermann, H. Rubira, and M. S. Sloth, Hot new early dark energy bridging cosmic gaps: Supercooled phase transition reconciles stepped dark radiation solutions to the Hubble tension with BBN, *Phys. Rev. D* **110**, 023531 (2024), arXiv:2404.07256 [astro-ph.CO].
- [31] E. Calabrese *et al.* (Atacama Cosmology Telescope), The Atacama Cosmology Telescope: DR6 constraints on extended cosmological models, *JCAP* **11**, 063, arXiv:2503.14454 [astro-ph.CO].
- [32] F. Niedermann and M. S. Sloth, New early dark energy, *Phys. Rev. D* **103**, L041303 (2021), arXiv:1910.10739 [astro-ph.CO].
- [33] F. Niedermann and M. S. Sloth, Resolving the Hubble tension with new early dark energy, *Phys. Rev. D* **102**, 063527 (2020), arXiv:2006.06686 [astro-ph.CO].
- [34] F. Niedermann and M. S. Sloth, Hot new early dark energy, *Phys. Rev. D* **105**, 063509 (2022), arXiv:2112.00770 [hep-ph].
- [35] F. Niedermann and M. S. Sloth, Hot new early dark energy: Towards a unified dark sector of neutrinos, dark energy and dark matter, *Phys. Lett. B* **835**, 137555 (2022), arXiv:2112.00759 [hep-ph].
- [36] D. E. Kaplan, G. Z. Krnjaic, K. R. Rehermann, and C. M. Wells, Atomic Dark Matter, *JCAP* **05**, 021, arXiv:0909.0753 [hep-ph].
- [37] F.-Y. Cyr-Racine and K. Sigurdson, Cosmology of atomic dark matter, *Phys. Rev. D* **87**, 103515 (2013), arXiv:1209.5752 [astro-ph.CO].
- [38] F.-Y. Cyr-Racine, F. Ge, and L. Knox, Symmetry of Cosmological Observables, a Mirror World Dark Sector, and the Hubble Constant, *Phys. Rev. Lett.* **128**, 201301 (2022), arXiv:2107.13000 [astro-ph.CO].

- [39] N. Blinov, G. Krnjaic, and S. W. Li, Toward a realistic model of dark atoms to resolve the Hubble tension, *Phys. Rev. D* **105**, 095005 (2022), arXiv:2108.11386 [hep-ph].
- [40] S. Bansal, J. Barron, D. Curtin, and Y. Tsai, Precision cosmological constraints on atomic dark matter, *JHEP* **10**, 095, arXiv:2212.02487 [hep-ph].
- [41] M. A. Buen-Abad, Z. Chacko, C. Kilic, G. Marques-Tavares, and T. Youn, Stepped partially acoustic dark matter, large scale structure, and the Hubble tension, *JHEP* **06**, 012, arXiv:2208.05984 [hep-ph].
- [42] S. Bansal, J. H. Kim, C. Kolda, M. Low, and Y. Tsai, Mirror twin Higgs cosmology: constraints and a possible resolution to the H_0 and S_8 tensions, *JHEP* **05**, 050, arXiv:2110.04317 [hep-ph].
- [43] M. A. Buen-Abad, Z. Chacko, C. Kilic, G. Marques-Tavares, and T. Youn, Stepped partially acoustic dark matter: likelihood analysis and cosmological tensions, *JCAP* **11**, 005, arXiv:2306.01844 [astro-ph.CO].
- [44] M. A. Buen-Abad, Z. Chacko, I. Flood, C. Kilic, G. Marques-Tavares, and T. Youn, Atomic dark matter, interacting dark radiation, and the Hubble tension, *JHEP* **07**, 084, arXiv:2411.08097 [hep-ph].
- [45] M. A. Buen-Abad, Z. Chacko, I. Flood, C. Kilic, G. Marques-Tavares, and T. Youn, Dark Matter-Dark Radiation Interactions and the Hubble Tension (2025), arXiv:2511.16554 [astro-ph.CO].
- [46] F.-Y. Cyr-Racine, R. de Putter, A. Raccanelli, and K. Sigurdson, Constraints on Large-Scale Dark Acoustic Oscillations from Cosmology, *Phys. Rev. D* **89**, 063517 (2014), arXiv:1310.3278 [astro-ph.CO].
- [47] Y. Mellier *et al.* (Euclid), Euclid. I. Overview of the Euclid mission, *Astron. Astrophys.* **697**, A1 (2025), arXiv:2405.13491 [astro-ph.CO].
- [48] D. Spergel *et al.*, Wide-Field Infrared Survey Telescope-Astrophysics Focused Telescope Assets WFIRST-AFTA 2015 Report (2015), arXiv:1503.03757 [astro-ph.IM].
- [49] S. R. Coleman and E. J. Weinberg, Radiative Corrections as the Origin of Spontaneous Symmetry Breaking, *Phys. Rev. D* **7**, 1888 (1973).
- [50] E. Witten, Cosmological Consequences of a Light Higgs Boson, *Nucl. Phys. B* **177**, 477 (1981).
- [51] H. Rubira, A. Mazoun, and M. Garny, Full-shape BOSS constraints on dark matter interacting with dark radiation and lifting the S_8 tension, *JCAP* **01**, 034, arXiv:2209.03974 [astro-ph.CO].

- [52] N. Schöneberg, G. Franco Abellán, T. Simon, A. Bartlett, Y. Patel, and T. L. Smith, Comparative analysis of interacting stepped dark radiation, *Phys. Rev. D* **108**, 123513 (2023), arXiv:2306.12469 [astro-ph.CO].
- [53] E. Camphuis *et al.* (SPT-3G), SPT-3G D1: CMB temperature and polarization power spectra and cosmology from 2019 and 2020 observations of the SPT-3G Main field (2025), arXiv:2506.20707 [astro-ph.CO].
- [54] C.-P. Ma and E. Bertschinger, Cosmological perturbation theory in the synchronous and conformal Newtonian gauges, *Astrophys. J.* **455**, 7 (1995), arXiv:astro-ph/9506072.
- [55] S. Bashinsky and E. Bertschinger, Position-space description of the cosmic microwave background and its temperature correlation function, *Phys. Rev. Lett.* **87**, 081301 (2001), arXiv:astro-ph/0012153.
- [56] D. Blas, J. Lesgourgues, and T. Tram, The Cosmic Linear Anisotropy Solving System (CLASS) II: Approximation schemes, *JCAP* **07**, 034, arXiv:1104.2933 [astro-ph.CO].
- [57] J. Torrado and A. Lewis, Cobaya: Code for Bayesian Analysis of hierarchical physical models, *JCAP* **05**, 057, arXiv:2005.05290 [astro-ph.IM].
- [58] N. Aghanim *et al.* (Planck), Planck 2018 results. VIII. Gravitational lensing, *Astron. Astrophys.* **641**, A8 (2020), arXiv:1807.06210 [astro-ph.CO].
- [59] L. Herold, E. G. M. Ferreira, and E. Komatsu, New Constraint on Early Dark Energy from Planck and BOSS Data Using the Profile Likelihood, *Astrophys. J. Lett.* **929**, L16 (2022), arXiv:2112.12140 [astro-ph.CO].
- [60] E. B. Holm, L. Herold, S. Hannestad, A. Nygaard, and T. Tram, Decaying dark matter with profile likelihoods, *Phys. Rev. D* **107**, L021303 (2023), arXiv:2211.01935 [astro-ph.CO].
- [61] J. S. Cruz, S. Hannestad, E. B. Holm, F. Niedermann, M. S. Sloth, and T. Tram, Profiling cold new early dark energy, *Phys. Rev. D* **108**, 023518 (2023), arXiv:2302.07934 [astro-ph.CO].
- [62] A. G. Adame *et al.* (DESI), Validation of the Scientific Program for the Dark Energy Spectroscopic Instrument, *Astron. J.* **167**, 62 (2024), arXiv:2306.06307 [astro-ph.CO].
- [63] W. Cvetko, M. Joseph, and G. Marques-Tavares, InterACTing dark radiation models after ACT (2025), arXiv:2512.19633 [astro-ph.CO].
- [64] M. Garny, F. Niedermann, and M. S. Sloth, in preparation.